Effects of a Liquid Layer on Thickness-Shear Vibrations of Rectangular AT-Cut Quartz Plates

Peter C. Y. Lee, *Member, IEEE*, and Rui Huang

Abstract—**Thickness-shear vibrations of a rectangular AT-cut quartz with one face in contact with a layer of Newtonian (linearly viscous and compressible) fluid are studied. The two-dimensional (2-D) governing equations for vibrations of piezoelectric crystal plates given previously are used in the present study. The solutions for 1-D shear wave and compressional wave in a liquid layer are obtained, and the stresses at the bottom of the liquid layer are used as approximations to the stresses exerting on the crystal surface in the plate equations.**

Closed form solutions are obtained for both free and piezoelectrically forced thickness-shear vibrations of a finite, rectangular AT-cut quartz in contact with a liquid layer of finite thickness. From the present solutions, a simple and explicit formula is deduced for the resonance frequency of the fundamental thickness-shear mode, which includes the effects of both shear and compressional waves in the liquid layer and the effect of the thickness-to-length ratio of the crystal plate. The formula reduces to the widely used frequency equation obtained by many previous investigators for infinite plates. The resonance frequency of a rectangular AT-cut quartz, computed as a function of the thickness of the adjacent liquid layer, agrees closely with the experimental data measured by Schneider and Martin.

I. Introduction

The utilization of thickness-shear mode (TSM) quartz crystal resonators as liquid-phase sensors has been studied for a long time [1]–[6]. The frequency equations for thickness-shear vibrations of quartz crystal plates of infinite extent in contact with a liquid layer have been obtained and widely used to predict the relationship between the change in resonance frequencies and the liquid properties, which assume that the shear displacement is uniform across the surface of the TSM resonator and only a shear wave is generated in the liquid layer. Until recently, the influences of compressional wave generation in the liquid layer due to the nonuniform thickness-shear motion in a finite quartz plate have been considered [6]–[8].

In the present article, the nonuniform thickness-shear vibrations of a finite, rectangular AT-cut quartz in contact with a liquid layer of finite thickness is studied. The effects of both shear and compressional waves in the liquid layer are considered.

The recently derived two-dimensional (2-D) equations for thickness-shear and flexural vibrations of piezoelectric crystal plates with electroded faces [9] are used for the AT-cut quartz plate. The normal and tangential stresses in the liquid layer subject to uniform oscillating boundary conditions are obtained from simplified governing equations for the Newtonian fluid (linearly viscous and compressible) by assuming small perturbations in fluid density and pressure. By requiring the continuity of displacements and stresses at the interface of the crystal plate and the liquid layer, the face tractions of the plate are expressed in terms of boundary stresses of the liquid layer. The resulting equations are further simplified by Tiersten's "thickness-shear approximation" [10]. Closed form solutions are obtained for both free and piezoelectrically forced thickness-shear vibrations. A simple and explicit formula for the resonance frequency of the fundamental thickness-shear mode is deduced, in which the effects of shear and compressional waves in the liquid layer and the effect of the thickness-to-length ratio of the plate are included. The resonance frequency is computed as a function of the thickness of the adjacent liquid layer and compared with the experimental data by Schneider and Martin [8].

II. First-Order 2-D Equations

Consider a rectangular AT-cut quartz plate with thickness $2b$ and length $2a$ as shown in Fig. 1. The surfaces of the plate at $x_2 = \pm b$ are fully covered by electrodes of thickness $2b'$ and mass density ρ'. A liquid layer of thickness h_L is in contact with the upper surface of the plate at $x_2 = b + 2b'$. The dimension of the plate in the x_3 direction is assumed to be infinite.

A set of first-order 2-D equations for vibrations of piezoelectric crystal plates with electroded faces was derived in [9]. For a rectangular AT-cut quartz, the equations for thickness-shear (TSh) and flexural (F) modes varying along the x_1 direction are reduced as follows:

$$\begin{aligned} u_1(x_1,x_2,t) &= -u_{2,1}^{(0)}(x_1,t)x_2 + u_1^{(1)}(x_1,t)\cos\left[\frac{\pi}{2}\left(1-\frac{x_2}{b}\right)\right], \\ u_2(x_1,x_2,t) &= u_2^{(0)}(x_1,t), \\ \phi(x_1,x_2,t) &= \bar{V}_0(t) + \bar{V}_1(t)\frac{x_2}{b} + \phi^{(2)}(x_1,t)\sin\left(\pi\frac{x_2}{b}\right), \end{aligned} \tag{1}$$

Manuscript received April 17, 2001; accepted December 11, 2001. This work was supported by Grant No. DAAH 04-95-0102 from the U.S. Army Research Office.

The authors are with the Department of Civil and Environmental Engineering, Princeton University, Princeton, NJ 08544 (e-mail: lee@princeton.edu).

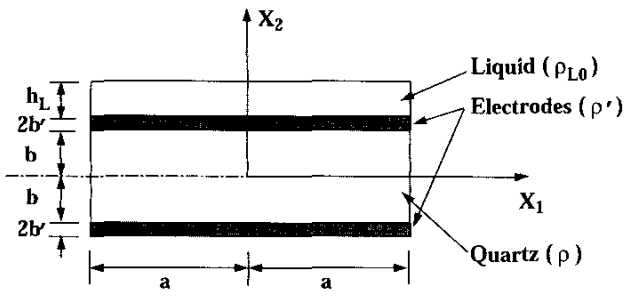

Fig. 1. A finite AT-cut quartz with electrodes and in contact with a liquid layer.

and

$$\begin{aligned}
&2c_{66}u_{1,1}^{(1)} + \mathcal{F}_2^{(0)} = 2(1+R)\rho b\ddot{u}_2^{(0)},\\
&c_{11}^{(1)}u_{1,11}^{(1)} - \left(\frac{\pi}{2b}\right)^2 c_{66}u_1^{(1)} - \frac{8b}{\pi^2}c_{11}^{(1)}u_{2,111}^{(0)}\\
&+\frac{8}{3\pi}e_{11}^{(1)}\phi_{,11}^{(2)} - \frac{2\pi}{3b^2}e_{26}\phi^{(2)} - \frac{2}{b^2}e_{26}\bar{V}_1 + \frac{1}{b}\mathcal{F}_1^{(1)}\\
&= (1+2R)\rho\ddot{u}_1^{(1)} - \frac{8}{\pi^2}\rho b\ddot{u}_{2,1}^{(0)},\\
&-\frac{2b}{\pi}e_{11}^{(1)}u_{2,111}^{(0)} + \frac{8}{3\pi}e_{11}^{(1)}u_{1,11}^{(1)} - \frac{2\pi}{3b^2}e_{26}u_1^{(1)}\\
&-\epsilon_{11}^{(1)}\phi_{,11}^{(2)} + \left(\frac{\pi}{b}\right)^2\epsilon_{22}\phi^{(2)} = 0,
\end{aligned} \tag{2}$$

where

$$\begin{aligned}
\mathcal{F}_j^{(n)} &= T_{2j}(x_2 = b + 2b') - (-1)^n T_{2j}(x_2 = -b - 2b'),\\
\bar{V}_1 &= \frac{1}{2}[\phi(x_2 = b) - \phi(x_2 = -b)],\\
\bar{V}_0 &= \frac{1}{2}[\phi(x_2 = b) + \phi(x_2 = -b)],
\end{aligned} \tag{3}$$

and

$$\begin{aligned}
c_{pq}^{(1)} &= c_{pq} - \frac{c_{p2}c_{2q}}{c_{22}},\\
e_{ip}^{(1)} &= e_{ip} - \frac{c_{p2}e_{i2}}{c_{22}},\\
\epsilon_{ij}^{(1)} &= \epsilon_{ij} + \frac{e_{i2}e_{j2}}{c_{22}},\\
R &= \frac{2\rho' b'}{\rho b}.
\end{aligned} \tag{4}$$

For plates in contact with a liquid layer, the coupled thickness-shear and flexural vibrations will generate both shear and compressional waves in the liquid layer, and both tangential and normal tractions are exerted on the plate surface, i.e., $\mathcal{F}_1^{(1)}$ and $\mathcal{F}_2^{(0)}$ in (2) are nonzero and related to the liquid layer.

III. Effects of a Liquid Layer

The governing equations of motion of a linearly viscous and compressible fluid consist of the continuity equation, the equation of motion, and the constitutive equation, i.e.,

$$\begin{aligned}
&\frac{d\rho_L}{dt} + \rho_L\nabla\cdot\mathbf{v} = 0,\\
&\rho_L\frac{d\mathbf{v}}{dt} = \nabla\cdot\mathbf{T} + \mathbf{f}_B,\\
&\mathbf{T} = -p\mathbf{I} + \mu(\nabla\mathbf{v} + \mathbf{v}\nabla) + \mathbf{I}\lambda(\nabla\cdot\mathbf{v}),
\end{aligned} \tag{5}$$

where ρ_L is the density of fluid, $\mathbf{f}_B$ is the body force per unit volume, $\mathbf{v}$ is the velocity vector, $\mathbf{T}$ is the stress tensor, p is the pressure in the fluid as a function of space and time, $\mathbf{I}$ is the identity tensor, μ and λ are the coefficients of viscosity. In fact, the second coefficient of viscosity λ is not well defined and the term $\lambda(\nabla\cdot\mathbf{v})$ is almost always so small that it is quite proper to simply ignore the effect of λ altogether [11].

In (5), we have 10 equations for 11 unknowns: ρ_L, p, $\mathbf{v}(3)$, $\mathbf{T}(6)$. The system is completed by including an equation of state, i.e., a relation between the change in density and the associated change in pressure. Although the equation of state of liquids is not known with sufficient precision to make the theoretical calculation practical, a simple relation can be obtained by defining the adiabatic compressibility coefficient as:

$$\beta_s = \frac{1}{\rho_L}\left(\frac{\partial\rho_L}{\partial p}\right)_s, \tag{6}$$

where s denotes that (6) is evaluated at constant entropy.

Assuming small oscillations about the equilibrium values of density and pressure, ρ_{L0} and p_0, we have:

$$\begin{aligned}
\rho_L &= \rho_{L0} + \rho_{Le}, \quad |\rho_{Le}| \ll \rho_{L0},\\
p &= p_0 + p_e, \quad |p_e| \ll p_0,
\end{aligned} \tag{7}$$

where ρ_{L0}, p_0 are considered constant by the homogeneous approximation [12], and ρ_{Le}, p_e are small disturbances. By substituting (7) into (6) and neglecting ρ_{Le} in comparison with ρ_{L0}, we obtain a relation between the disturbances:

$$\rho_{Le} = \beta_s\rho_{L0}p_e. \tag{8}$$

By substituting (8) into $(7)_1$ and, in turn, into $(5)_1$ and neglecting the convective term in the material derivative $\frac{d\rho_L}{dt}$, we obtain:

$$\beta_s\dot{p}_e + \nabla\cdot\dot{\mathbf{u}} = 0, \tag{9}$$

where $\mathbf{u}$ is the displacement vector in the fluid, and a dot on top means $\frac{\partial}{\partial t}$. Integrating (9) with respect to time gives:

$$p_e = -\frac{1}{\beta_s}\nabla\cdot\mathbf{u}. \tag{10}$$

By substituting (10) into $(7)_2$, $(5)_3$, and in turn, into $(5)_2$, and neglecting the body force and the convective

term in the material derivative $\frac{d\mathbf{v}}{dt}$, we obtain a linear displacement equation of motion for liquids:

$$\rho_{L0}\ddot{\mathbf{u}} = \frac{1}{\beta_s}\nabla(\nabla\cdot\mathbf{u}) + (\mu+\lambda)\nabla(\nabla\cdot\dot{\mathbf{u}}) + \mu\nabla^2\dot{\mathbf{u}}. \tag{11}$$

By taking the divergence of (11), we have:

$$\rho_{L0}\nabla\cdot\ddot{\mathbf{u}} = \frac{1}{\beta_s}\nabla^2(\nabla\cdot\mathbf{u}) + (2\mu+\lambda)\nabla^2(\nabla\cdot\dot{\mathbf{u}}), \tag{12}$$

which is a wave equation of $\nabla\cdot\mathbf{u}$ for liquids with viscous damping. The wave velocity of $\nabla\cdot\mathbf{u}$ without damping is:

$$c_0 = \sqrt{\frac{1}{\rho_{L0}\beta_s}}, \tag{13}$$

which is the sound velocity in liquids.

A. Shear Wave in Liquids

It was pointed out by Stokes [13], that it is possible to produce a transverse shear wave in a viscous liquid, even without the presence of shear elasticity. Assume that the liquid is disturbed by the harmonic motion of a plate attached to the bottom face of the liquid layer and oscillating in the x_1 direction. Because u_1 is the only nonzero displacement component and it depends on x_2 and t only, (11) reduces to:

$$\rho_{L0}\ddot{u}_1 = \mu\frac{\partial^2\dot{u}_1}{\partial x_2^2}. \tag{14}$$

By assuming that u_1 being a harmonic function of the time with angular frequency ω, we obtain the general solution of (14):

$$u_1 = \{A\exp[-(1+i)\kappa_s x_2] + B\exp[(1+i)\kappa_s x_2]\}\, e^{i\omega t}, \tag{15}$$

where κ_s is the attenuation coefficient of the shear wave given by:

$$\kappa_s = \frac{1}{\delta} = \sqrt{\frac{\rho_{L0}\omega}{2\mu}}, \tag{16}$$

and δ is the decay length of the shear wave in the viscous fluid.

The stress in the liquid is obtained by substituting (15) into (10) and $(5)_3$. It follows that p_e is zero and the only nonzero shearing stress T_{21} is given by:

$$T_{21} = (1-i)\omega^{3/2}\sqrt{\frac{\rho_{L0}\mu}{2}}\{A\exp[-(1+i)\kappa_s x_2] - B\exp[(1+i)\kappa_s x_2]\}e^{i\omega t}. \tag{17}$$

The constants A and B are determined by applying appropriate boundary conditions. As shown in Fig. 1, the liquid layer with thickness h_L occupies the region $b+2b' < x_2 < b+2b'+h_L$. Assuming that there is no slip between the liquid and the plate and that the surface of the liquid layer at $x = b+2b'+h_L$ is traction-free, we have:

$$\begin{aligned} u_1 &= \bar{u}_1 e^{i\omega t}, \quad \text{at } x_2 = b+2b', \\ T_{21} &= 0, \quad \text{at } x_2 = b+2b'+h_L, \end{aligned} \tag{18}$$

where $\bar{u}_1$ is the amplitude of the oscillation of the plate at the bottom face of the liquid layer.

By substituting (15) and (17) into (18) and solving for A and B, we obtain the shearing stress exerted on the plate at the bottom of the liquid layer as:

$$T_{21}(x_2 = b+2b') = (1-i)\omega^{3/2} \times \sqrt{\frac{\rho_{L0}\mu}{2}}\tanh[(1+i)\kappa_s h_L]\bar{u}_1 e^{i\omega t}. \tag{19}$$

We see from (16) that κ_s is large or the decay length δ is small in the case the liquid has a small viscosity μ and the frequency ω is moderate. Accordingly, the displacement u_1 in (15) is damped out in a very short distance from the lower boundary and the effect of wave reflection from the upper surface of the liquid layer becomes insignificant as long as [14]

$$\kappa_s h_L = \frac{h_L}{\delta} \gg 1. \tag{20}$$

Under the condition (20), $\tanh[(1+i)\kappa_s h_L] \approx 1$ and, therefore, the shearing stress T_{21} in (19) also becomes almost independent of h_L and the boundary condition at the upper surface of the liquid layer.

B. Compressional Wave in Liquids

Similarly, if a plane attached to the bottom face of the liquid layer oscillates in the x_2 direction, a 1-D compressional wave is generated in the liquid. In this case, the motion of the liquid is only in x_2 direction and depends on x_2 and t only. Hence, (11) becomes:

$$\rho_{L0}\ddot{u}_2 = \rho_{L0}c_0^2\frac{\partial^2 u_2}{\partial x_2^2} + (2\mu+\lambda)\frac{\partial^2\dot{u}_2}{\partial x_2^2}. \tag{21}$$

Again, assuming that u_2 is a harmonic function of the time with angular frequency ω, we obtain the general solution of (21):

$$u_2 = \left[Ae^{-i\zeta_c x_2} + Be^{i\zeta_c x_2}\right]e^{i\omega t}, \tag{22}$$

where

$$\zeta_c^2 = \frac{\rho_{L0}\omega^2}{\rho_{L0}c_0^2 + i\omega(2\mu+\lambda)}. \tag{23}$$

Note that ζ_c is complex for viscous liquids, which means that the compressional wave propagates with damping in the viscous liquids. For the liquids with small viscosity, (23) can be approximated by:

$$\zeta_c = \frac{\omega}{c_0}\left[1 - i\omega\frac{2\mu+\lambda}{2\rho_{L0}c_0^2}\right]. \tag{24}$$

By substituting (22) into (10) and then into $(5)_3$, we obtain the normal stress in the liquid:

$$T_{22} = -\frac{i\rho_{L0}\omega^2}{\zeta_c}\left[Ae^{-i\zeta_c x_2} - Be^{i\zeta_c x_2}\right] e^{i\omega t}. \tag{25}$$

For a liquid layer with a traction-free upper surface, we have:

$$\begin{aligned} u_2 &= \bar{u}_2 e^{i\omega t}, \quad \text{at } x_2 = b + 2b', \\ T_{22} &= 0, \quad \text{at } x_2 = b + 2b' + h_L, \end{aligned} \tag{26}$$

where $\bar{u}_2$ is the amplitude of the plane boundary at the bottom of the liquid layer.

By substituting (22) and (25) into (26) and solving for A and B, we obtain the normal stress exerted on the plate at the bottom of the liquid layer as:

$$T_{22}(x_2 = b + 2b') = \frac{\rho_{L0}\omega^2}{\zeta_c}\tan(\zeta_c h_L)\bar{u}_2 e^{i\omega t}. \tag{27}$$

Alternatively, for a liquid layer with a rigid plane boundary at the upper surface, instead of (26) we have:

$$\begin{aligned} u_2 &= \bar{u}_2 e^{i\omega t}, \quad \text{at } x_2 = b + 2b', \\ u_2 &= 0, \quad \text{at } x_2 = b + 2b' + h_L. \end{aligned} \tag{28}$$

In a similar manner, we obtain the normal stress exerted on the plate at the bottom of the liquid layer:

$$T_{22}(x_2 = b + 2b') = -\frac{\rho_{L0}\omega^2}{\zeta_c}\mathrm{c}\tan(\zeta_c h_L)\bar{u}_2 e^{i\omega t}. \tag{29}$$

C. Face Tractions on Crystal Plates

For a plate vibrating in the coupled thickness-shear and flexural modes, both shear and compressional waves are generated in the adjacent liquid layer, and they should be coupled to each other. However, we may assume this coupling to be negligible so that the analysis of the 1-D uncoupled shear and compressional waves in the preceding two subsections can be used to obtain approximately the face tractions exerted on the crystal by the liquid layer.

By requiring the continuity of displacements at the interface of the crystal plate and the liquid layer and disregarding the deformation of electrodes, we have, from (1) and (18), (26),

$$\begin{aligned} \bar{u}_1 e^{i\omega t} &= u_1^{(1)} - b u_{2,1}^{(0)}, \\ \bar{u}_2 e^{i\omega t} &= u_2^{(0)}. \end{aligned} \tag{30}$$

By substituting (30) into (19) and (27) or (29), requiring the continuity of tractions at the interface, and using the definition of $\mathcal{F}_j^{(n)}$ in (3), we obtain:

$$\begin{aligned} \mathcal{F}_1^{(1)} &= (1-i)\tanh[(1+i)\kappa_s h_L]\omega^{3/2}\sqrt{\frac{\rho_{L0}\mu}{2}}(u_1^{(1)} - b u_{2,1}^{(0)}), \\ \mathcal{F}_2^{(0)} &= \mathcal{L}_c \rho_{L0} h_L \omega^2 u_2^{(0)}, \end{aligned} \tag{31}$$

where $\mathcal{L}_c$ depends upon the boundary condition at the upper surface of the liquid layer as:

$$\begin{aligned} \mathcal{L}_c &= \frac{\tan(\zeta_c h_L)}{\zeta_c h_L} \text{ for traction free surface,} \\ \mathcal{L}_c &= -\frac{\mathrm{c}\tan(\zeta_c h_L)}{\zeta_c h_L} \text{ for rigid surface.} \end{aligned} \tag{32}$$

Thus, effects of the liquid layer on vibrations of the crystal plate are accommodated by inserting (31) into the 2-D plate equations in (2).

IV. Thickness-Shear Approximation

For AT-cut quartz of infinite extent in x_1 and x_3 directions, the 2-D equations in (2) can be reduced to one single equation for simple thickness-shear vibrations:

$$\left[1 + \frac{16}{9\pi^2}\frac{e_{26}^2}{c_{66}\epsilon_{22}} - (1-i)\mathcal{L}_s\left(\frac{\omega}{\omega_1}\right)^{3/2}\right]\left(\frac{\pi}{2b}\right)^2 c_{66} u_1^{(1)} + (1+2R)\rho\ddot{u}_1^{(1)} + \frac{2}{b^2}e_{26}\bar{V}_1 = 0, \tag{33}$$

where

$$\begin{aligned} \mathcal{L}_s &= \frac{2}{\pi}\sqrt{\frac{\rho_{L0}\mu\omega_1}{2\rho c_{66}}}\tanh\left[(1+i)\kappa_s h_L\right], \\ \omega_1 &= \frac{\pi}{2b}\sqrt{\frac{c_{66}}{\rho}}. \end{aligned} \tag{34}$$

By setting $\bar{V}_1$ to zero and $u_1^{(1)}$ to be a harmonic function of time with angular frequency ω, we obtain the frequency equation:

$$(1+2R)\rho\omega^2 - \left[1 + \frac{16}{9\pi^2}\frac{e_{26}^2}{c_{66}\epsilon_{22}} - (1-i)\mathcal{L}_s\left(\frac{\omega}{\omega_1}\right)^{3/2}\right]\left(\frac{\pi}{2b}\right)^2 c_{66} = 0. \tag{35}$$

From (35), we obtain a complex resonance frequency for the fundamental simple thickness-shear vibrations of AT-cut quartz, which can be approximately written as:

$$\Omega = \frac{\omega}{\omega_1} = 1 - R + \frac{8}{9\pi^2}\frac{e_{26}^2}{c_{66}\epsilon_{22}} - \frac{1}{2}\mathcal{L}_s(1-i). \tag{36}$$

We see in (36) that the effects from the mass of electrodes, piezoelectric stiffening, and viscous liquid layer are represented by the second, third, and fourth terms, respectively. By inserting (34) into the last term of (36), which is complex, we see that its real part decreases the frequency and the imaginary part reduces the quality factor of the resonator. Results similar to (36) have been obtained and widely used by many as those of [1]–[6].

For AT-cut quartz of finite extent, the thickness-shear mode is always coupled with flexural mode in (2). For frequencies confined in a narrow range centered at the fundamental thickness-shear resonance and for small wave

numbers, $(2)_1$ can be eliminated by applying Tiersten's thickness-shear approximation method [10] to the present case of study.

First, by following [10], we let $\omega \approx \omega_1$ and $\mathcal{F}_2^{(0)} = 0$ in $(2)_1$ and solve for $u_2^{(0)}$:

$$u_2^{(0)} = -\frac{4b}{\pi^2(1+R)} u_{1,1}^{(1)}. \tag{37}$$

Then, by inserting (37) into $(31)_2$ for $\mathcal{F}_2^{(0)}$, which is nonzero for plate in contact with a liquid layer, and further substituting the resulting expression of $\mathcal{F}_2^{(0)}$ back into $(2)_1$, we obtain the modified displacement component

$$u_2^{(0)} = -\frac{4b}{\pi^2(1+R)} u_{1,1}^{(1)} \left(1 - \frac{\mathcal{L}_c R_L}{1+R}\right), \tag{38}$$

where

$$R_L = \frac{\rho_{L0} h_L}{2\rho b}. \tag{39}$$

Finally, substitution of (38) into $(2)_2$ and omission of the $u_{2,111}^{(0)}$ term in $(2)_3$ lead to the governing equations for an AT-cut quartz in contact with a liquid layer under the thickness-shear approximation:

$$\begin{aligned}
&\left[c_{11}^{(1)} + (1-i)\mathcal{L}_s c_{66}\right] u_{1,11}^{(1)} - \left(\frac{\pi}{2b}\right)^2 c_{66}\left[1 - (1-i)\mathcal{L}_s\right] u_1^{(1)} \\
&\quad + \frac{8}{3\pi} e_{11}^{(1)} \phi_{,11}^{(2)} - \frac{2\pi}{3b^2} e_{26} \phi^{(2)} - \frac{2}{b^2} e_{26} \bar{V}_1 \\
&\quad = (1+2R)\rho \ddot{u}_1^{(1)} + \frac{32\rho b^2}{\pi^4(1+R)} \ddot{u}_{1,11}^{(1)} \left(1 - \frac{\mathcal{L}_c R_L}{1+R}\right), \qquad (40) \\
&\frac{8}{3\pi} e_{11}^{(1)} u_{1,11}^{(1)} - \frac{2\pi}{3b^2} e_{26} u_1^{(1)} - \epsilon_{11}^{(1)} \phi_{,11}^{(2)} + \left(\frac{\pi}{b}\right)^2 \epsilon_{22} \phi^{(2)} = 0.
\end{aligned}$$

In Sections V and VI, closed form solutions are obtained from (40) for free and piezoelectrically forced vibrations of finite plates.

V. Free Vibrations

By setting $\bar{V}_1$ to zero for free vibrations with shorted electrodes, letting:

$$\begin{aligned}
u_1^{(1)} &= bA_1 \cos(\xi x_1) e^{i\omega t}, \\
\phi^{(2)} &= b\sqrt{\frac{c_{66}}{\epsilon_{22}}} A_2 \cos(\xi x_1) e^{i\omega t},
\end{aligned} \tag{41}$$

and substituting (41) into (40), we obtain:

$$\sum_{j=1}^{2} Q_{ij}(X,\Omega) A_j = 0, \quad i,j = 1,2, \tag{42}$$

where

$$\begin{aligned}
Q_{11} &= \mathcal{C}_1 - \mathcal{C}_2 X^2, \\
Q_{12} &= Q_{21} = -\frac{8}{3\pi}(\bar{e}_{26} + \bar{e}_{11}^{(1)} X^2), \\
Q_{22} &= 4 + \bar{\epsilon}_{11}^{(1)} X^2,
\end{aligned} \tag{43}$$

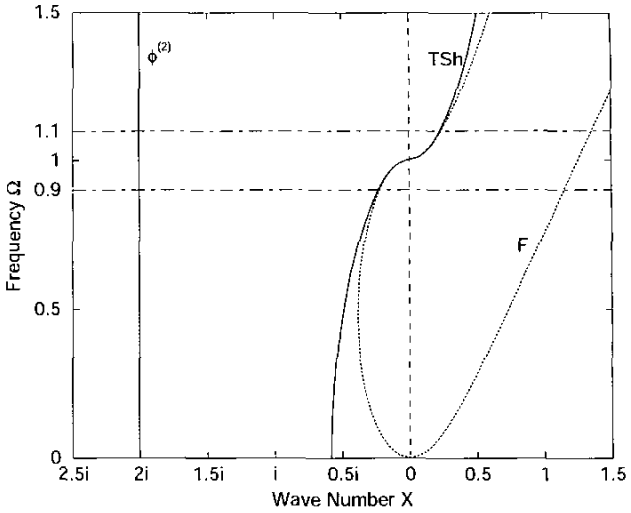

Fig. 2. Comparison of dispersion curves for thickness-shear vibrations of an AT-cut quartz with $R = 0$ and $h_L = 0$. Solid lines are from the 2-D equations with thickness-shear approximation. Dotted lines are from the 2-D equations of coupled thickness-shear and flexural vibrations.

and

$$\begin{aligned}
X &= \frac{2\xi b}{\pi}, \Omega = \frac{\omega}{\omega_1}, \\
\mathcal{C}_1 &= (1+2R)\Omega^2 - 1 + (1-i)\mathcal{L}_s, \\
\mathcal{C}_2 &= \bar{c}_{11}^{(1)} + (1-i)\mathcal{L}_s + \frac{8\Omega^2}{\pi^2(1+R)} \left(1 - \frac{\mathcal{L}_c R_L}{1+R}\right), \\
\bar{c}_{11}^{(1)} &= \frac{c_{11}^{(1)}}{c_{66}}, \bar{\epsilon}_{11}^{(1)} = \frac{\epsilon_{11}^{(1)}}{\epsilon_{22}}, \\
\bar{e}_{26} &= \frac{e_{26}}{\sqrt{c_{66}\epsilon_{22}}}, \bar{e}_{11}^{(1)} = \frac{e_{11}^{(1)}}{\sqrt{c_{66}\epsilon_{22}}}.
\end{aligned} \tag{44}$$

For nontrivial solutions to (42), we have:

$$\det[Q_{ij}(X,\Omega)] = 0, \tag{45}$$

which gives the dispersion relation of thickness-shear vibrations.

For a given value of Ω, (45) yields two roots,

$$X_j = \frac{2}{\pi}\xi_j b, \quad j = 1,2, \tag{46}$$

where X_1 denotes the wave number corresponding to thickness-shear displacement $u_1^{(1)}$ and X_2 the wave number to electric potential $\phi^{(2)}$. The dispersion curves computed from (45) for an AT-cut quartz without electrodes ($R = 0$) and with no liquid in contact ($h_L = 0$) are plotted as solid lines in Fig. 2. Dispersion curves also are computed from (2), the equations without using the thickness-shear approximation to eliminate $u_2^{(0)}$, and shown by dotted lines in Fig. 2 for comparison. We see, in Fig. 2, that the two sets of curves for $u_1^{(1)}$ and $\phi^{(2)}$ are very close and X_1 is very small for a range of frequency in the vicinity of $\Omega = 1$.

In order to satisfy edge conditions of finite plates, both roots X_j or ξ_j of (45) are needed for general solutions. Hence, we let:

$$u_1^{(1)} = b\sum_{j=1}^{2}\alpha_{1j}B_j\cos(\xi_j x_1)e^{i\omega t},$$
$$\phi^{(2)} = b\sqrt{\frac{c_{66}}{\epsilon_{22}}}\sum_{j=1}^{2}\alpha_{2j}B_j\cos(\xi_j x_1)e^{i\omega t}, \tag{47}$$

where α_{ij} are the ratios of amplitudes and satisfy:

$$\sum_{k=1}^{2}Q_{ik}(X_j,\Omega)\alpha_{kj} = 0, \quad i,j = 1,2. \tag{48}$$

For plates with fixed displacement and charge-free edges, we require:

$$u_1^{(1)} = \bar{D}_1^{(2)} = 0, \quad \text{at } x_1 = \pm a, \tag{49}$$

where $\bar{D}_1^{(2)}$ is a 2-D charge density, for which the constitutive equation is given by $(39)_7$ of [9] as:

$$\bar{D}_1^{(2)} = \frac{2b}{\pi}e_{11}^{(1)}u_{2,11}^{(0)} + \frac{8}{3\pi}e_{11}^{(1)}u_{1,1}^{(1)} - \epsilon_{11}^{(1)}\phi_{,1}^{(2)}. \tag{50}$$

By substituting (47) into (50) and then into (49), we obtain:

$$\begin{bmatrix}\alpha_{11}\cos\left(\frac{\pi a}{2b}X_1\right) & \alpha_{12}\cos\left(\frac{\pi a}{2b}X_2\right)\\ \beta_1\sin\left(\frac{\pi a}{2b}X_1\right) & \beta_2\sin\left(\frac{\pi a}{2b}X_2\right)\end{bmatrix}\begin{pmatrix}B_1\\B_2\end{pmatrix} = 0, \tag{51}$$

where

$$\beta_j = X_j\left[-\frac{4}{3}\alpha_{1j}\bar{e}_{11}^{(1)} + \frac{\pi}{2}\alpha_{2j}\bar{\epsilon}_{11}^{(1)}\right]. \tag{52}$$

Vanishing of the determinant of the coefficient matrix of (51) gives a transcendental equation for resonance frequencies:

$$\cot\left(\frac{\pi a}{2b}X_1\right) = \frac{\alpha_{11}\beta_2}{\alpha_{12}\beta_1}\cot\left(\frac{\pi a}{2b}X_2\right). \tag{53}$$

As we can see from the dispersion curves in Fig. 2, $X_1 \ll 1$ and $X_2 \approx 2i$. By the definitions of α_{ij} and β_j, it can be shown that the right-hand side of (53) is very small and can be approximated by zero. Then, from the left-hand side of (53), we have:

$$X_1 \approx \frac{nb}{a}, \quad n = 1,3,5,\cdots. \tag{54}$$

For the fundamental thickness-shear mode, $n = 1$, hence:

$$X_1 \approx \frac{b}{a}. \tag{55}$$

We see from (55) that the prior requirement of X_1 to be small under the thickness-shear approximation is satisfied for thin plates.

By substituting (55) into (45), imposing the condition (20), neglecting higher-order terms of small quantities, and solving for the resonance frequency of the fundamental thickness-shear mode, we obtain:

$$\Omega = 1 - R + \frac{8}{9\pi^2}\frac{e_{26}^2}{c_{66}\epsilon_{22}} + \left(\frac{4}{\pi^2} + \frac{1}{2}\frac{c_{11}^{(1)}}{c_{66}} + \frac{16}{9\pi^2}\frac{e_{26}e_{11}^{(1)}}{c_{66}\epsilon_{22}}\right)\frac{b^2}{a^2} - \frac{1}{2}(1-i)\mathcal{L}_s - \frac{4}{\pi^2}\frac{b^2}{a^2}\frac{\mathcal{L}_c R_L}{1+\frac{8}{\pi^2}\frac{b^2}{a^2}\mathcal{L}_c R_L}. \tag{56}$$

It may be seen from (56) that effects of the edge conditions of a finite plate are given by the two terms that are proportional to $(b/a)^2$, the square of the thickness-to-length ratio of the plate. As the length of the plate becomes longer and longer (i.e., as $a \to \infty$), (56) reduces to (36). We note that in (56) the fourth term represents mainly the effect of flexural stiffness of the plate and the last term contains the effect of the compressional wave in the liquid layer through the factor $\mathcal{L}_c R_L$, which are given in (32) and (39) for either traction-free or rigid-displacement conditions at the upper surface of the liquid layer.

We define the frequency change by:

$$\Delta f = f - f_0, \tag{57}$$

where f and f_0 denote the thickness-shear frequencies of the plate with and without the liquid layer, respectively. The real part of Δf is computed from (56) as a function of h_L for a rectangular AT-cut quartz with $R = 0$, $2a = 10.16$ mm, $2b = 0.33$ mm and in contact with a layer of water ($\rho_{L0} = 998.2$ kg/m^3, $\mu = 1.002$ mPa·s, $\lambda = 0$, $c_0 \approx 1500$ m/s), for which the upper surface is assumed to be in contact with a rigid plane and thus $(32)_2$ is used for $\mathcal{L}_c$. Predicted results are compared with the experimental data of Schneider and Martin [8], as shown in Fig. 3. Although the experiments were conducted for circular disks of AT-cut quartz, it may be seen in Fig. 3 that the agreement is close, especially for the periodical characteristics of the response. We note that the reflection of the compressional wave contributes to the cyclical variation. We see from (24) and (32) that the period of the variation is approximately $\pi c_0/\omega$, which equals to half wave length of the sound wave in the liquid. In Fig. 3, the dotted line is computed from (36); therefore, it represents the frequency change of an infinite plate or that of a finite plate without taking into account the effect of compressional waves.

VI. Piezoelectrically Forced Vibrations

Consider the thickness-shear vibrations piezoelectrically forced by an alternating potential, $\phi = \pm\phi_0 e^{i\omega t}$, applied across the electrodes at $x_2 = \pm b$. By $(3)_{2,3}$, we have $\bar{V}_1 = \phi_0 e^{i\omega t}$ and $\bar{V}_2 = 0$. The complete solution of (40) consists of two parts: the homogeneous solution for $\bar{V}_1 = 0$ and a particular solution accommodating the nonzero $\bar{V}_1$.

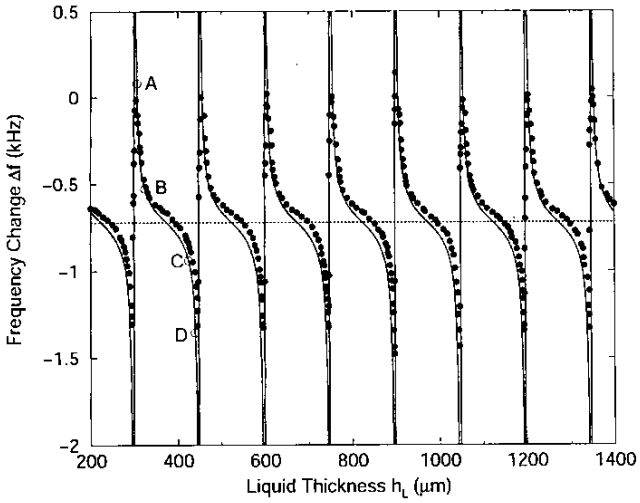

Fig. 3. Comparison of predicted changes in the fundamental thickness-shear frequency Δf (solid lines) with the experimental data of Schneider and Martin [8] (dots) for an AT-cut quartz in contact with a layer of water of varying thickness h_L.

The homogeneous solution is the same as (47), the solution obtained in the previous section for free vibrations. For the particular solution, we let:

$$u_1^{(1)} = \gamma\sqrt{\frac{\epsilon_{22}}{c_{66}}}\phi_0 e^{i\omega t}, \quad \phi^{(2)} = \frac{2}{3\pi}\gamma\bar{e}_{26}\phi_0 e^{i\omega t}, \tag{58}$$

where

$$\gamma = \frac{8\bar{e}_{26}}{\pi^2\left[(1+2R)\Omega^2 - 1 - \frac{16}{9\pi^2}\bar{e}_{26}^2 + (1-i)\mathcal{L}_s\right]}. \tag{59}$$

Thus, the complete solution for piczoelectrically forced vibrations is:

$$u_1^{(1)} = \left[\gamma + \sum_{j=1}^{2}\alpha_{1j}B_j\cos(\xi_j x_1)\right]\sqrt{\frac{\epsilon_{22}}{c_{66}}}\phi_0 e^{i\omega t},$$
$$\phi^{(2)} = \left[\frac{2}{3\pi}\gamma\bar{e}_{26} + \sum_{j=1}^{2}\alpha_{2j}B_j\cos(\xi_j x_1)\right]\phi_0 e^{i\omega t}. \tag{60}$$

Substituting (60) into the edge condition (49), we obtain:

$$\begin{bmatrix}\alpha_{11}\cos\left(\frac{\pi a}{2b}X_1\right) & \alpha_{12}\cos\left(\frac{\pi a}{2b}X_2\right)\\ \beta_1\sin\left(\frac{\pi a}{2b}X_1\right) & \beta_2\sin\left(\frac{\pi a}{2b}X_2\right)\end{bmatrix}\begin{pmatrix}B_1\\B_2\end{pmatrix} = \begin{pmatrix}-\gamma\\0\end{pmatrix}. \tag{61}$$

where β_j are given by (52).

Once the coefficients B_1 and B_2 are solved from (61), the displacement and electric potential can be computed from (60).

The total surface charge on the electroded surface of an area $2a \times 2c$ is:

$$Q = \frac{\pi}{2}c\int_{-a}^{a}\bar{D}_2^{(1)}\,dx_1, \tag{62}$$

and the constitutive equation for the 2-D charge density $\bar{D}_2^{(1)}$ is given by $(39)_5$ of [9] as:

$$\bar{D}_2^{(1)} = \frac{\pi}{2b}e_{26}u_1^{(1)} - \frac{4}{3b}\epsilon_{22}\phi^{(2)} - \frac{4}{\pi b}\epsilon_{22}\bar{V}_1. \tag{63}$$

By substituting (60) into (63) and then into (62), we obtain:

$$Q = \frac{4ac}{b}\epsilon_{22}\phi_0\left[1 - \left(\frac{\pi^2}{8} - \frac{2}{9}\right)\bar{e}_{26}\gamma - \sum_{j=1}^{2}\left(\frac{\pi^2}{8}\bar{e}_{26}\alpha_{1j} - \frac{\pi}{3}\alpha_{2j}\right)B_j\frac{\sin\xi_j a}{\xi_j a}\right]e^{i\omega t}. \tag{64}$$

Hence, the motional capacitance is:

$$C_m = \frac{Q}{2\bar{V}_1} = C_s\left[1 - \left(\frac{\pi^2}{8} - \frac{2}{9}\right)\bar{e}_{26}\gamma - \sum_{j=1}^{2}\left(\frac{\pi^2}{8}\bar{e}_{26}\alpha_{1j} - \frac{\pi}{3}\alpha_{2j}\right)B_j\frac{\sin\xi_j a}{\xi_j a}\right], \tag{65}$$

and the admittance:

$$Y_m = i\omega C_m, \tag{66}$$

where C_s is the static capacitance defined by:

$$C_s = \epsilon_{22}\frac{2ac}{b}. \tag{67}$$

We note that the motional capacitance in (65) is complex due to the damping effect of the viscous liquid layer. We define the capacitance ratio C_r as the real part of C_m divided by C_s, i.e.,

$$C_r = \mathrm{Re}\left(\frac{C_m}{C_s}\right), \tag{68}$$

and obtain the motional conductance G_m from the real part of the admittance:

$$G_m = \mathrm{Re}(i\omega C_m). \tag{69}$$

Both C_r and G_m are computed and plotted in Fig. 4 as functions of the forcing frequency f for the AT-cut quartz and for four different values of h_L corresponding to the four points labeled as A, B, C, and D in Fig. 3. For the case of the quartz with no liquid in contact (i.e., $h_L = 0$), the capacitance ratio C_r is represented by the curve E in Fig. 4, and the corresponding motional conductance G_m is zero because no damping is present. If we define the resonance frequency as the forcing frequency at which G_m is a maximum or $C_r = 1$, then we see the changes of resonance frequencies from Fig. 4 agree with the corresponding points in Fig. 3. It may be seen in Fig. 4 that the maximum values of G_m remain almost constant with respect to h_L. It is because the damping effect is mainly from the shear wave in the liquid and as noted earlier that under the condition (20) the effect of the shear wave is almost independent of h_L.

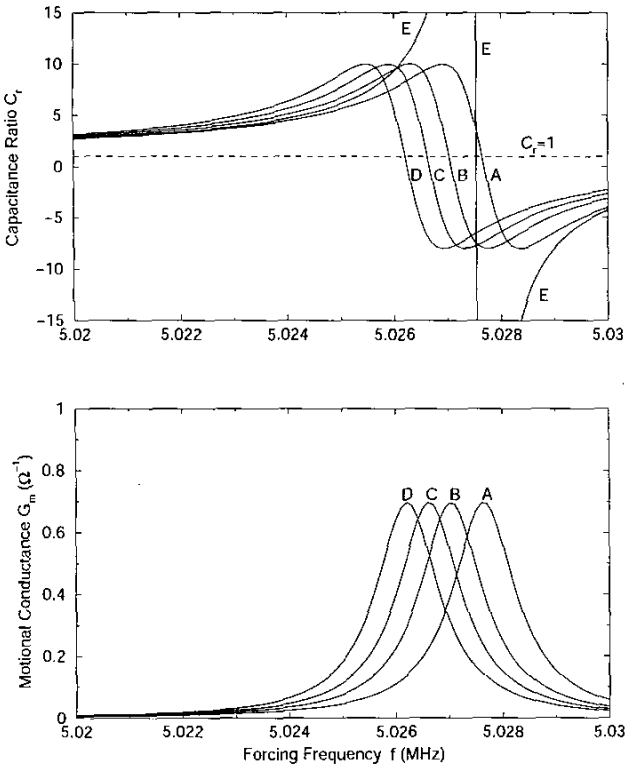

Fig. 4. Computed capacitance ratio and motional conductance as functions of forcing frequency for a rectangular AT-cut quartz in contact with a layer of water of thickness h_L. A: $h_L = 306\ \mu m$, B: $h_L = 325\ \mu m$, C: $h_L = 425\ \mu m$, D: $h_L = 440\ \mu m$, E: $h_L = 0$.

VII. Conclusions

Nonuniform thickness-shear vibrations of a finite, rectangular AT-cut quartz in contact with a viscous and compressible liquid layer are studied. Solutions are obtained for free and piezoelectrically forced vibrations with fixed displacement and charge-free edge conditions.

A simple and explicit formula for the fundamental thickness-shear frequency is deduced, which includes the effects of the mass of electrodes, the piezoelectric stiffening, the thickness-to-length ratio of the plate, and the liquid layer. Effects from both shear and compressional waves in the liquid layer are considered. The computed resonance frequency as a function of the thickness of the liquid layer agrees closely with the experimental data of Schneider and Martin [8]. The viscous damping effect is contributed mainly by the shear wave in the liquid through the viscosity coefficient μ, and it is independent of the liquid thickness h_L as long as $h_L \gg \delta$, where δ is the decay length of the shear wave. The compressional wave, which is essentially generated by the flexural motion of the plate, causes a periodic change in the resonance frequency with a period depending on the operating frequency and the sound velocity in the liquid. The effect of the compressional wave depends upon the thickness-to-length ratio of the plate and diminishes to zero as the plate length approaches infinity.

References

[1] K. K. Kanazawa and J. G. Gordon, II, "The oscillation frequency of a quartz resonator in contact with a liquid," *Anal. Chim. Acta*, vol. 175, pp. 99–105, 1985.

[2] C. E. Reed, K. K. Kanazawa, and J. H. Kaufman, "Physical description of a viscoelastically loaded AT-cut quartz resonator," *J. Appl. Phys.*, vol. 68, pp. 1993–2001, 1990.

[3] F. Josse, Z. A. Shana, D. E. Radtke, and D. T. Haworth, "Analysis of piezoelectric bulk-acoustic-wave resonators as detectors in viscous conductive liquids," *IEEE Trans. Ultrason., Ferroelect., Freq. Contr.*, vol. 37, pp. 359–368, 1990.

[4] S. J. Martin, G. C. Frye, and K. O. Wessendorf, "Sensing liquid properties with thickness-shear mode resonators," *Sens. Actuators A*, vol. 44, pp. 209–218, 1994.

[5] M. Thompson and G. Hayward, "Mass response of the thickness-shear mode acoustic wave sensor in liquids as a central misleading dogma," in *Proc. IEEE Int. Freq. Contr. Symp.*, 1997, pp. 114–119.

[6] R. Thalhammer, S. Braun, B. Devcic-Kuhar, M. Gröschl, F. Trampler, E. Benes, H. Nowotny, and M. Kostal, "Viscosity sensor utilizing a piezoelectric thickness shear sandwich resonator," *IEEE Trans. Ultrason., Ferroelect., Freq. Contr.*, vol. 45, pp. 1331–1340, 1998.

[7] Z. Lin and M. D. Ward, "The role of longitudinal waves in quartz crystal microbalance applications in liquids," *Anal. Chem.*, vol. 67, pp. 685–693, 1995.

[8] T. W. Schneider and S. J. Martin, "Influence of compressional wave generation on thickness-shear mode resonator response in a fluid," *Anal. Chem.*, vol. 67, pp. 3324–3335, 1995.

[9] P. C. Y. Lee, J. D. Yu, and W. S. Lin, "A new two-dimensional theory for vibrations of piezoelectric crystal plates with electroded faces," *J. Appl. Phys.*, vol. 83, pp. 1213–1223, 1998.

[10] H. F. Tiersten, *Linear Piezoelectric Plate Vibrations*. New York: Plenum, 1969, pp. 183–201.

[11] F. M. White, *Viscous Fluid Flow*, 2nd ed. New York: McGraw-Hill, 1991, pp. 59–68.

[12] R. N. Thurston, "Wave propagation in fluids and normal solids," *Phys. Acoust.*, vol. 1(A), pp. 1–110, 1964.

[13] L. Rayleigh, *Theory of Sound*, 2nd ed., vol. 2. New York: Dover, 1945, p. 317.

[14] R. B. Lindsay, *Mechanical Radiation*. New York: McGraw-Hill, 1960, pp. 351–354.

Rui Huang received his B.S. and M.Eng. degrees in mechanics and mechanical engineering from the University of Science and Technology of China (USTC) in 1994 and 1996, respectively, and his Ph.D. degree in civil and environmental engineering from Princeton University in 2001. He is now a research associate at the Civil and Environmental Engineering Department and Princeton Materials Institute of Princeton University.

Dr. Huang's research interests include high-frequency vibrations of piezoelectric crystal plates, smart materials and structures, evolving material structures of small feature sizes, thin films, and other micro/nano-structures.